Novel Method To Enlarge the Surface Area of SBA-15

Montserrat Colilla, Francisco Balas, Miguel Manzano, and María Vallet-Regí*

Departamento de Química Inorgánica, Facultad de Farmacia, Universidad Complutense de Madrid, 28040 Madrid, Spain

Received April 16, 2007
Revised Manuscript Received May 16, 2007

Silica-based ordered mesoporous materials have attracted much attention in recent years because of their porous structures with siloxane walls and narrow pore size distributions.[1,2] These materials have been used to host chemicals[3] or drugs[4,5] with different shapes, sizes, and functionalities. Therefore, the development of novel techniques to improve the adsorption characteristics of ordered mesoporous materials would be of great interest for current applications. Much effort is being dedicated to increase the number of available mesostructures by varying the templating agent and synthesis conditions,[6] as well as modifying the chemistry at the interface between silica and surfactant.[7] In this way, mixing strong and polyprotic weaker acids, like H_3PO_4, would promote changes in the ionic strength at the interface. These variations could improve the surface properties of the final materials because the inorganic framework is affected by the nature of the interaction with the surfactant molecules. In addition, the incorporation of phosphorus species as acid centers[8] have been proposed for mesoporous frameworks for applications in electronics,[9] catalysis,[10] and biomaterial science.[11]

In this work, the synthesis of hexagonally ordered SBA-15 mesoporous silica through the addition of H_3PO_4 is reported. The synthesis procedure involves the use of Pluronic P123 ($EO_{20}PO_{70}EO_{20}$; BASF) as the template agent, which is dissolved in distilled water and variable amounts of HCl (37%) and/or H_3PO_4 (85%) (Aldrich) obtaining initial solutions with the following molar compositions: 1:0.017:*n*:*x*:208 SiO_2/P123/H_3PO_4/HCl/H_2O, where $n = 1.5$, 2.2, 4.5, and 6.5 and $x = 3.4$ for HP_n and $x = 0$ for P_n materials. The silica source was tetraethyl orthosilicate (TEOS, Aldrich), and it was added to the surfactant acid solutions without earlier purification. Solutions were stirred at 308 K for 24 h in sealed Teflon beakers and subsequently placed at 373 K for 24 h. Every solution was filtered, washed, and finally dried at 363 K for 12 h in air. Template removal was performed by calcination in air using two succesive steps, first heating at 523 K for 3 h and then at 823 K for 4 h. For comparison, conventional SBA-15, using a one-step calcination at 823 K, was also synthesized. The total amount of P incorporated was analyzed by X-ray fluorescence (XRF), revealing that the amount of P in samples with $n \leq 4.5$ was less than 0.2 wt %. In contrast, P contents for $HP_{6.5}$ and $P_{6.5}$ samples were 5.0 and 7.6 wt %, respectively.

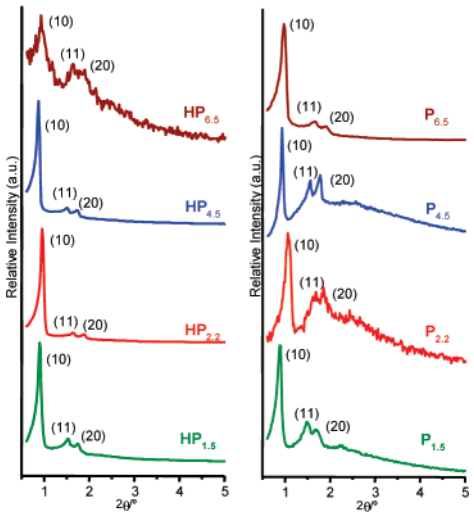

Figure 1. SA-XRD patterns of HP_n and P_n samples.

Small-angle X-ray diffraction patterns (SA-XRD) of HP_n and P_n (Figure 1) materials showed three clear maxima, which are assigned to the (10), (11), and (20) reflections of a hexagonal planar symmetry (*p*6*mm*). Figure 1 shows that for HP_n samples, high H_3PO_4 contents during synthesis induce a broadening of the XRD maxima, and there is a significant amount of amorphous phase. Alternatively, for P_n samples, the increase in the amount of H_3PO_4 in the synthesis induces more defined hexagonal symmetry of mesopores.

Surface analysis by N_2 adsorption shows a very large increase in the total gas adsorbed for the HP_n samples with respect to the conventional SBA-15 silica (Figure 2). As a common feature in hexagonally ordered mesoporous silica, all materials exhibit type IV isotherms, and the shape of the hysteresis loops points to cylindrical mesopores with very narrow pore size distributions.[12]

* To whom correspondence should be addressed. E-mail: vallet@farm.ucm.es.

(1) (a) Kresge, C. T.; Leonowicz, M. E.; Roth, W. J.; Vartulli, J. C.; Beck, J. S. *Nature* **1992**, *359*, 710. (b) Inagaki, S.; Fukushima, Y.; Kuroda, K. *Chem. Commun.* **1993**, 680. (c) Zhao, D. Y.; Feng, J. L.; Huo, Q. S.; Melosh, N.; Fredricksson, G. H.; Chmelka, B. F.; Stucky, G. D. *Science* **1998**, *279*, 548.
(2) Thomas, J. M.; Johnson, B. F. G.; Raja, R.; Samkar, G.; Midgley, P. A. *Acc. Chem. Res.* **2003**, *36*, 20.
(3) Schüth, F.; Schmidt, W. *Adv. Mater.* **2002**, *14*, 629.
(4) (*a*) Vallet-Regí, M.; Rámila, A.; del Real, R. P.; Pérez-Pariente, J. *Chem. Mater.* **2001**, *13*, 308. (*b*) Balas, F.; Manzano, M.; Horcajada, P.; Vallet-Regí, M. *J. Am. Chem. Soc.* **2006**, *128*, 8116.
(5) Vallet-Regí, M. *Chem.—Eur. J.* **2006**, *12*, 5934.
(6) Hoffmann, F.; Cornelius, M.; Morell, J.; Fröba, M. *Angew. Chem., Int. Ed.* **2006**, *45*, 3216.
(7) (a) Zhang, W.; Glomski, B.; Pauly, T. R.; Pinnavaia, T. J. *Chem. Commun.* **1999**, 1803. (b) Tanev, P. T.; Pinnavaia, T. J. *Science* **1995**, *267*, 865.
(8) Corriu, R. J. P.; Hoarau, C.; Mehdi, A.; Reyé, C. *Chem. Commun.* **2000**, 71.
(9) Pang, J. B.; Qiu, K. Y.; Wei, Y.; Lei, X. J.; Liu, Z. F. *Chem. Commun.* **2000**, 477.
(10) (a) Herrera, J. M.; Reyes, J.; Roquero, P.; Klimova, T. *Microporous Mesoporous Mater.* **2005**, *83*, 283. (b) Pitchumani, R.; Li, W.; Coppens, M.O. *Catal. Today* **2005**, *105*, 618.
(11) Vallet-Regí, M.; Ruiz-González, L.; Izquierdo-Barba, I.; González-Calbet, J. M. *J. Mater. Chem.* **2006**, *16*, 26.
(12) Gregg S. J.; Sing, K. S. W. *Adsorption, Surface Area and Porosity*, 2nd ed.; Academic Press: New York, 1982.

10.1021/cm071032p CCC: $37.00
Published on Web 06/01/2007

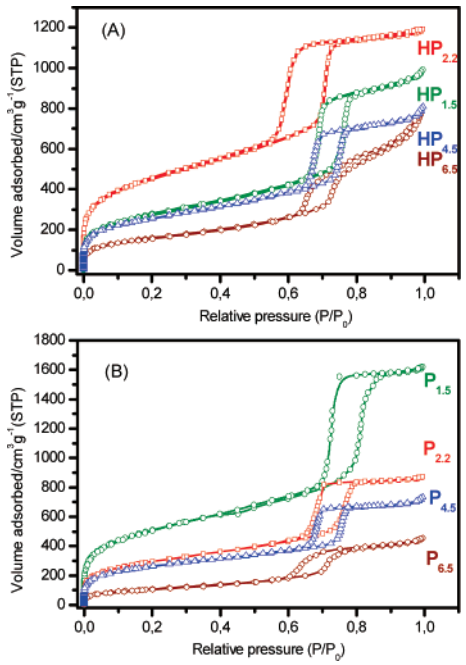

Figure 2. N_2 adsorption isotherms at 77 K for HP_n and P_n samples.

Table 1. Porosity Data of the Synthesized Mesoporous Materials[a]

sample	ρ_S, g/cm^3	S_{BET}, m^2/g	V_T, cm^3/g	$V_{\mu P}$, cm^3/g	V_{mP}, cm^3/g	d_{10}, nm	D_P, nm	t_{wall}, nm
SBA-15	2.2	702	0.99	0.04	0.91	9.5	9.3	1.7
SBA-15 (HP_0)	2.2	1001	1.34	0.05	1.10	9.7	9.8	1.4
$HP_{1.5}$	2.2	1007	1.47	0.05	1.13	9.8	9.9	1.4
$HP_{2.2}$	1.8	1605	1.84	0.13	1.68	9.1	9.3	1.2
$HP_{4.5}$	2.0	909	1.25	0.06	0.97	10.0	9.7	1.9
$HP_{6.5}$	2.1	582	1.19	0.01	0.86	9.1	9.3	1.2
$P_{1.5}$	1.5	1830	2.48	0.13	2.19	10.0	10.4	1.2
$P_{2.2}$	1.7	1069	1.35	0.07	1.17	8.2	8.0	1.5
$P_{4.5}$	2.1	906	1.13	0.07	0.96	9.4	9.1	1.8
$P_{6.5}$	2.2	393	0.71	0.01	0.48	9.2	8.0	2.7

[a] ρ_S: skeletal density measured by using He pycnometry. d_{10}: SA-XRD spacing of the (10) reflection of a hexagonal plane array of pores. D_P: mesopore width calculated using the KJS procedure[13]. t_{wall}: silica wall thickness between adjacent mesopores.

The data in Table 1 show that there is an increase in total pore volume (V_T) of HP_n and P_n samples when $n < 6.5$. This is essentially due to the enlargement of the mesopore volume (V_{mP}) though there is a slight increase in the micropore volume ($V_{\mu P}$) estimated after *t*-plots. Surface areas determined by the BET method (S_{BET}) are also larger than for conventional SBA-15, which is attributed to the growth of V_{mP}. The method employed for the template removal also plays an important role in the textural properties of the final materials. During the first stage, using relatively low calcination temperature prevents the silica matrix from shrinking.[14] This leads to a retention of the original sizes and volumes of the micro- and mesopores.

For $HP_{6.5}$ there is a reduction in both V_T and S_{BET} that could be attributed to the amorphous phase that was detected after XRD analysis. The increase in V_{mP} and S_{BET} is noteworthy for P_n samples (Figure 2), where a clear correlation between the amount of H_3PO_4 employed for synthesis and the surface data could be established. $V_{\mu P}$ is comparable to that observed for conventional SBA-15, although the decrease in the microporous participation with the increase in the amount of H_3PO_4 is interesting to note. Moreover, skeletal densities (ρ_S, measured by using He pycnometry) of the materials with larger S_{BET} and V_{mP} are considerably smaller than for conventional SBA-15 materials or P-containing samples. This fact could point to the formation of mesoporous frameworks with a lower polymerization degree.[15]

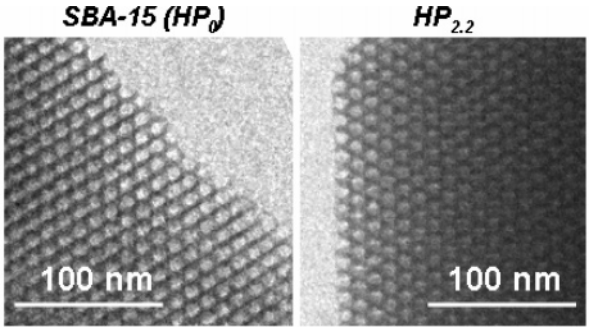

Figure 3. TEM micrographs of SBA-15 (HP_0) and $HP_{2.2}$ materials.

The characteristic two-dimensional hexagonal arrays of pores of this type of mesoporous materials were confirmed by transmission electron microscopy (TEM). Figure 3 shows a *p6mm* symmetry with unit cell parameters of 11.6 and 10.7 nm, for HP_0 and $HP_{2.2}$ samples, respectively. The phosphoric acid catalyst induces a small reduction of the cell parameter, which is in agreement with the similar pore size reduction that has been observed by the KJS calculations of the pore volume data (Table 1).[13]

To clarify the nature of the interactions between surfactant and H_3PO_4, Fourier transform infrared (FTIR) spectra of the aqueous blends of P123 and acids with the same composition of samples before adding TEOS were investigated (see Supporting Information). The shifts of the FTIR stretching vibration bands of two types of bonds, C−O from surfactant and P−OH from H_3PO_4, confirm the interaction between the polar head of the surfactant and the acid. As it was reported for neutral P123, the silica−surfactant interface is of the $N^0(I^-X^+)$ type,[16] and the partial charge promoted on polyether chains by the H_3PO_4 modification would induce a different rate on the evolution of the micellar structure. This last effect has been previously reported by Ruthstein *et al.*,[17] who studied the initial formation stages of SBA-15 using spin-labeled block copolymer templates and several acids.

Phosphate molecules located among micelles could modify the ionic strength and pH of the environment and induce a different interaction type, more related to the N^0I^0 type.[18]

(13) Kruk, M.; Jaroniec, M.; Sayari, A. *Chem. Mater.* **1999**, *11*, 492.
(14) (a) Yang, C. M.; Zibrowius, B; Schmidt, W.; Schüth, F. *Chem. Mater.* **2003**, *15*, 3739. (b) Yang, C. M.; Zibrowius, B.; Schmidt, W.; Schüth, F. *Chem. Mater.* **2004**, *16*, 2918.
(15) Iler, R. K. *The Chemistry of Silica*; Wiley-Interscience: New York, 1979.
(16) (a) Huo, Q.; Margolese, D. I.; Ciesla, U.; Feng, P.; Gier, T. E.; Sieger, P.; Leon, R.; Petroff, P. M.; Schüth, F.; Stucky, G. D. *Nature* **1994**, *368*, 317. (b) Soler-Illia, G. J. A. A.; Sanchez, C.; Lebeau, B.; Patarin, J. *Chem. Rev.* **2002**, *102*, 4093.
(17) (a) Ruthstein, S.; Frydman, V.; Kababya, S.; Landau, M.; Goldfarb, D. *J. Phys. Chem. B* **2003**, *107*, 1739. (b) Ruthstein, S.; Schmidt, J.; Kesselman, E.; Talmon, Y.; Goldfarb, D. *J. Am. Chem. Soc.* **2006**, *128*, 3366.
(18) Attard, G. S.; Glyde, J. C.; Göltner, C. *Nature* **1995**, *378*, 366.

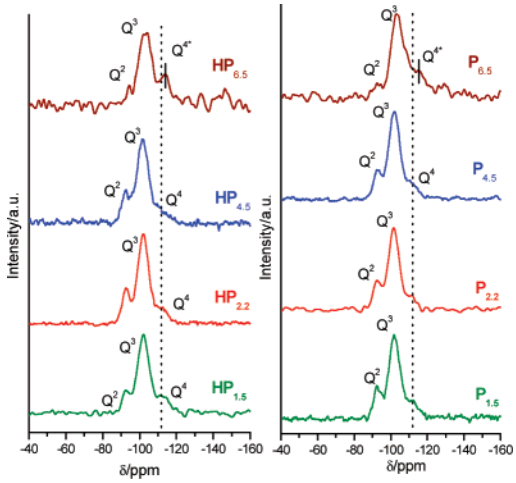

Figure 4. ^{29}Si CP-MAS/NMR spectra of HP_n and P_n materials.

Scheme 1. Mechanism Proposed for the Formation of Mesoporous Structures Using Non-Ionic Surfactant (P123) and Different Acid Media

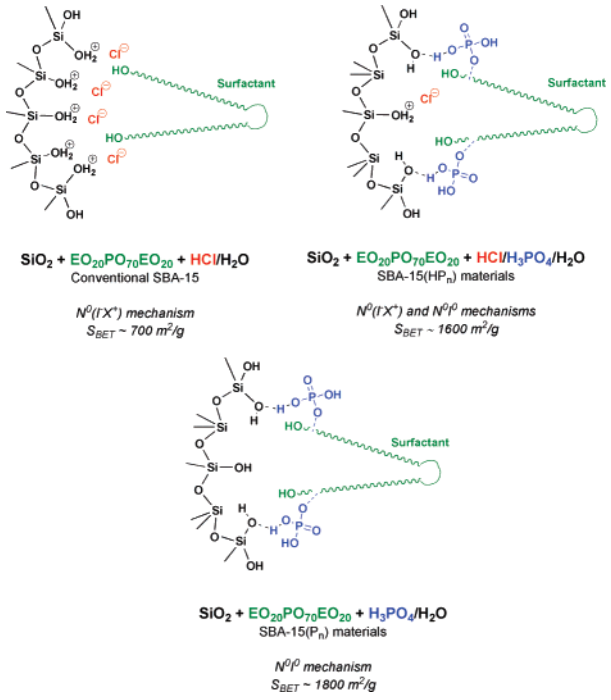

This fact would result in materials with different textural properties depending on the composition. These proposed mechanisms are displayed in Scheme 1.

For establishing the chemical nature of the silica networks ^{29}Si cross-polarization magic-angle-spinning (CP-MAS)/NMR spectra of samples were recorded. As it can be observed in Figure 4, ^{29}Si NMR spectra of phosphorus-free materials display bands around −92 ppm (Q^2), −102 ppm (Q^3), and −110 ppm (Q^4). In the NMR spectra of samples containing phosphorus ($HP_{6.5}$ and $P_{6.5}$), Q^2 and Q^3 signals are slightly shifted to negative values appearing at around

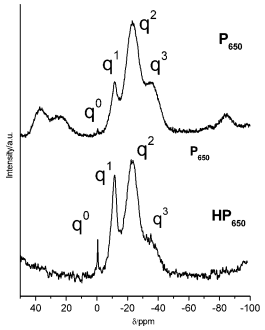

Figure 5. ^{31}P CP-MAS/NMR spectra of $HP_{6.5}$ and $P_{6.5}$ materials.

−93 ppm and −103 ppm, respectively. This chemical shift could suggest the incorporation of the phosphorus into the silica network. This fact agrees with the appearance of a new band at approximately −115 ppm, which could be related to $Si(OSi)_{4-x}(OP)_x$ with $x = 1-3$ (Q^4*) indicating that the P atoms would be cross-linked with the silicate matrix. In those cases where P was incorporated into the silica network, it would be interesting to determine the actual state of PO_4 units in the matrix. Furthermore, the ^{31}P NMR spectrum displayed in Figure 5 shows three clear bands at −11 ppm (q^1), −23 ppm (q^2), and −36 ppm (q^3), which are respectively due to O═P(OH)$_2$(OP, OSi), O═P(OH)(OP, OSi)$_2$, and O═P(OP)$_n$(OSi)$_m$.[19] In addition two paired sets of spinning sidebands of these peaks occur at $\delta = +37/+29$ ppm and $\delta = -74/-84$ ppm in the NMR spectrum of the $P_{6.5}$ material. NMR studies suggest the cross-linking of PO_4 and SiO_4 units forming the matrix. The incorporation of these phosphate centers could be responsible of the surface area reduction for $HP_{6.5}$ and $P_{6.5}$.

The use of H_3PO_4 together with HCl as catalysts for the templated formation during the sol−gel synthesis of ordered silica mesostructures produces an increase in the surface area and mesoporous volume of the obtained materials up to double those of conventional SBA-15. Finally, the improved surface properties of the synthesized ordered mesoporous silicas makes these materials excellent candidates for obtaining drug delivery systems that could be used in a large number of biomedical applications.

Acknowledgment. The authors thank Dr. I. Izquierdo-Barba and Prof. Osamu Terasaki for the TEM measurements. Financial support by Spanish CICYT (MAT 2005-01486 project) and CAM S-0505-MAT-0324 are also acknowledged.

Supporting Information Available: Synthesis and analysis techniques (XRD, XRF, FTIR, and N_2 adsorption; PDF). This material is available free of charge via the Internet at http://pubs.acs.org.

CM071032P

(19) (a) Eswaramoorthy, N. M.; Rao, C. N. R. *Mater. Res. Bull.* **1998**, *33*, 1549. (b) Szu, S. P.; Klein, L. C.; Greenblatt, M. *J. Non-Cryst. Solids* **1992**, *143*, 21.